J Mater Sci (2014) 49:2832–2843
DOI 10.1007/s10853-013-7989-y

Study of the hydrophobization of TEMPO-oxidized cellulose gel through two routes: amidation and esterification process

A. Benkaddour · C. Journoux-Lapp · K. Jradi · S. Robert · C. Daneault

Received: 15 October 2013 / Accepted: 21 December 2013 / Published online: 7 January 2014

Abstract In this paper, we studied the hydrophobization of TEMPO-oxidized cellulose gel (TOCgel) by covalent coupling of long carbon chains via esterification and amidation processes. In this context, amidation process was achieved by covalent coupling of stearylamine (SA) on the carboxyl moieties of TOCgel using carbodiimide and hydroxysuccimide as catalyst and amidation agent. In parallel, esterification process was realized by grafting of alkyl ketene dimer (AKD) on the hydroxyl groups of TOCgel in the presence of 1-methylimidazole as a promoter. The grafting state of the final products obtained under heterogeneous conditions was confirmed by fourier transform infrared spectroscopy (FTIR), X-ray photoelectron spectroscopy (XPS), thermogravimetric analysis (TGA), transmission and scanning electron microscopy, and contact angle measurement (CAM). The hydrophobic behavior of the obtained products was discussed based on the results of CAM and absorption rate of water drop in their film surface. FTIR and XPS results indicated the formation of amide bonding for the SA-g-TOCgel (amidation), and β-keto ester linkages for the AKD-g-TOCgel (esterification). As confirmed by CAM, the both chemical treatments enhanced the transition hydrophilic/hydrophobic behavior of the TOCgel fibers. It appeared also that CA values of grafted samples showed a slightly greater hydrophobicity of AKD-g-TOCgel (115° ± 2°) relatively to SA-g-TOCgel (102° ± 2°). However, the absorption rate of water drop seems to be relatively faster for AKD-g-TOCgel than for SA-g-TOCgel. Indeed, the water resistance of amidation product could be due to the high graft efficiency obtained (46.3 %) in comparison with that of the esterification product (30 %). In parallel, this result was confirmed by the dispersion test of modified TOCgels in hexane solvent which indicated clearly the high stable dispersion of SA-g-TOCgel obtained through the amidation process. Moreover, TGA result demonstrated that the thermal stability was found to be slightly higher for SA-g-TOCgel than for AKD-g-TOCgel. Finally, the excellent hydrophobic properties of modified TOCgel material could be suitable to be used as reinforcement for nonpolar polymer matrices in industrial applications.

A. Benkaddour · C. Journoux-Lapp · K. Jradi (✉) · S. Robert
Lignocellulosic Material Research Centre, Université du Québec à Trois-Rivières, 3351 Des Forges, Trois-Rivières, QC G9A 5H7, Canada
e-mail: khalil.jradi@uqtr.ca

C. Daneault
Canada Research Chair in Value-Added Paper, Université du Québec à Trois Rivières, 3351 Des Forges, Trois-Rivières, QC G9A 5H7, Canada

Introduction

In recent years, the use of cellulose nanofibers presents a great potential as a nanosized reinforcements for a large number of industrial applications ranging from fluids with specific rheological properties to the processing of nanocomposites [1, 2]. It includes also the reinforcement of composite materials, tissue engineering scaffolds, moistening masks for cosmetic applications, thickening agents, rheology modifiers, and adsorbents, paper reinforcement [3]. Because cellulose is an abundant, renewable, and biodegradable resource and having good mechanical properties, it is advantageous to utilize cellulosic nanofibers as reinforcement in such biocomposites in order to improve their thermal, optical, and mechanical properties even at relatively low filler contents [4, 5]. In fact, cellulose is part of an architectural edifice complex which varies

with the organism, the individual cellulose chains are associated by hydrogen bonds into nanofibers having diameters between 2 and 20 nm and lengths ranging from 100 nm to several micrometers depending on their biological origin [19]. Different types of cellulose nanofibers have been produced by other physical and chemical treatments of cellulose fibers. Sulfuric acid hydrolysis is known to produce cellulose nanowhiskers [20]. Powerful fibrillation using grinding [21], and homogenizing [22] devices were also reported to produce cellulose nanofibers. The advantage of the TEMPO oxidation process versus other techniques in the preparation of nanocellulose is due to several parameters. First, mechanical treatment requires a large amount of energy, and the resulting products consist mainly of bundles of microfibrils, and it is not possible to separate individual cellulose microfibrils. Second, the acid hydrolytic treatment can depolymerise the cellulose chains to yield a dramatic decrease in the microfibrils length and width which is not advantageous, since it damages the structure of the microfibrils [23]. For these reasons, we investigated the potential of the TEMPO oxidation method. It is known to introduce carboxylate moieties on the cellulose structure in order to improve chemical modification of cellulose nanofibers through the presence of carboxylate groups created by the TEMPO oxidation, and to preserve the micrometric length of the cellulose nanofibers (including both the crystalline and amorphous domains). Despite the advantageous of the TEMPO-oxidized nanocellulose as reinforcement material, there are some limitations. The most important restraint is the poor compatibility between the hydrophilic nanofiber and the hydrophobic polymer matrix [6, 7]. Hence, the fiber-matrix interface is usually the weakest point in a biocomposite, which makes the performance of the final composite limited by fiber pull-out rather than fiber break [6]. Thus, the full strength of the cellulose nanofiber as reinforcing material is not utilized, the optimal properties of the biocomposites are not obtained, and the full commercial potential is, therefore, not achieved. In order to overcome this problem, and consequently to improve the interfacial adhesion in the final composite, the hydrophilic character of cellulose nanofibers should be modified to make it more compatible with nonpolar matrices.

Over the last decades, surface modification (i.e., hydrophobization) of different celluloses has been accomplished via both chemical and physical modification using low-molecular-weight compounds and polymers [8–10]. Some of the chemical approaches involved the use of ring opening polymerization [11, 12], the atom transfer radical polymerization [13, 14], and also the use of the bifunctionnal bridge [15–17] onto the surface of the cellulose fibers. Furthermore, some chemical processes such as acid chloride, anhydrides, silanes, or isocyanates have been used in the grafting of small molecules onto the surface of cellulose nanocrystals NCC and cellulose nanofibrillated NFC [18]. However, only few work has been reported on the chemical hydrophobization onto the surface of TEMPO-oxidized nanocellulose. At the same time, the effectiveness of these chemical treatments in the hydrophobic behavior of the modified cellulose nanofibers is still poorly investigated.

Indeed, the target of our work was to investigate the grafting state of two sizing agents on the TEMPO-oxidized cellulose gel (TOCgel) through (i) the amidation with an alkylamine (SA) and (ii) the esterification with an alkyl ketene dimer (AKD) under heterogeneous conditions and using the same weight ratio of TOCgel/sizing agent (1:1 w/w). A comparison based on the obtained hydrophobic properties of final modified TOCgel will be discussed.

Experimental section

Materials

Stearylamine SA (C18, 99 %), alkyl ketene dimer AKD (mixture of stearic and palmitic acids, 60–40 % by weight), *N*-ethyl-*N*′-(3-dimethylaminopropyl) carbodiimide hydrochloride (EDAC), *N*-hydroxysuccinimide (NHS), sodium bromide (NaBr), sodium hypochlorite (NaOCl), and 4-acetamido-TEMPO (2,2,6,6-tetramethylpiperidin-1-oxyl) were purchased from Sigma Aldrich and used as received. A commercial never-dried bleached kraft wood pulp was used as the cellulose sample for the production of TOCgel through the TEMPO-mediated oxidation and mechanical treatments. Analytical grade chemicals and solvents were always used as received without further purification.

Production of TEMPO-oxidized cellulose gel

In the first step, the oxidation of native cellulose fibers was carried out by the TEMPO-mediated oxidation system [24] and conducted in a 45L flow-through sonoreactor (semi-continuous mode) with a nominal input power capacity of 2000 W (262 W/L, 12300 W/m^2), according to the procedure described [25, 26]. The sonoreactor is commercially available from Ultrasonic Power Corporation (USA) and is made from 316L stainless steel. Before oxidation, 400 g of dried bleached pulp was pre-soaked for 1 day in 40 l of deionized water at room temperature. The soaked pulp was disintegrated for 10 min in a laboratory disintegrator to obtain a uniform fiber suspension of about 1 % consistency. To the cellulose suspension, we added 9.2 g of 4-acetamido-TEMPO and 25 g of sodium bromide. A solution of NaOCl (3.1 mmol/g) was added dropwise to the mixture at room temperature under gentle agitation during

the first 30 min. The pH was maintained at 10.5 by adding 0.5 M NaOH. After the pH was stabilized, the reaction was stopped after 90 min by adding 1 l of H_2O_2 (1 %), and the pH was adjusted to 7 by adding 0.5 M NaOH or HCl as required. The TEMPO-oxidized product was filtered, washed thoroughly with deionized water, and stored at 4 °C. Then, the carboxylate content of the TEMPO-oxidized cellulose was determined using an electrical conductivity titration method [24], and it was equal to ~1150 mmol/kg. The obtained carboxylate celluloses were used to make the oxidized nanocellulose gel.

In the second step, TEMPO-oxidized cellulose gel (TOCgel nanofibers) was prepared by high shear dispersion of oxidized pulp in a wet colloid milling apparatus (MK 2000/4) from IKA Works, Inc. (USA). Briefly, the oxidized pulp suspension (2L) was pumped from an agitated tank between a conical rotor and a stator in the MK mill. In this work, the mill was operated in closed loop for a given amount of time (1 h) under the optimized operating conditions : The normal operating conditions of this laboratory setup were: 3 % consistency, 0.073 mm gap, 200 ml/min recirculation rate, 25 °C, and pH 7 [25]. Moreover, carboxylate groups created on the cellulose microfibrils by the TEMPO-mediated oxidation have anionic charges in water. These charges include electrostatic repulsions between the microfibrils which consequently help the disintegration process and contribute to the formation of individual microfibrils [27].

Hydrophobization of TOCgel

Stearylamine grafted TOCgel (amidation process)

In order to perform the amidation reaction between the stearylamine and TOCgel nanofibers, we used the NHS/EDC-mediated coupling procedure developed in previous researches with minor modifications [28–30]. Briefly, TOCgel (0.5 g) was pre-swelled in 100 ml of deionized water at room temperature. NHS (3.10^{-3} mol) and EDC (3.10^{-3} mol) were dissolved in deionized water, added to the above suspension, and mixed under moderate magnetic stirring. The mixture was continually stirred at room temperature for 30 min, while keeping the pH at 5 by adding 0.5 M NaOH and/or HCl. After that, 0.5 g of SA solution (pre-dissolved in ethanol) was added, and the pH of the mixture was adjusted to 8. The reaction was still under stirring at room temperature for 3 h.

The obtained suspension was then washed two times with deionized water, two times with HCl 0.1 M (protonation of residual carboxylate groups), two times with ethanol (to remove the unreacted SA), one time with deionized water, and finally dialyzed in deionized water to remove excess EDAC, NHS, and by-product urea by changing the surrounding water every 5 h. The resulted SA grafted TOCgel suspension was freeze dried and stored to be characterized by different techniques.

Alkyl ketene dimer grafted TOCgel (esterification process)

In the esterification treatment, freeze dried TOCgel nanofibers (0.5 g) were pre-swelled in 100 ml of DMAC solvent preheated at 70 °C and stirred for 20 min. 2 ml of MEI (promoter agent) was slowly added to the mixture and still stirred for 1 h. To the reaction medium, 0.5 g of AKD was added and the mixture was stirred at 70 °C for 3 h. Then, the mixture was cooled to room temperature, washed two times with toluene, three times with ethanol, two times with deionized water to remove excess AKD and all by-products. The resulted AKD grafted TOCgel was dried at ambient air and stored to be characterized by different techniques.

Characterization

Fourier transform infrared spectrometry (FTIR)

FTIR spectra were collected using a PerkinElmer 2000 Fourier transform infrared (FT-IR) spectrometer in transmission mode. 1 mg of dried sample and 100 mg crystalline KBr were ground together using an alumina mortar and pestle and pressed to form discs. A total of 16 scans were taken per sample with a resolution of 4 cm^{-1} (4000–400 cm^{-1}).

Transmission electron microscopy (TEM)

Transmission electron microscopy images of our samples were recorded using a Philips EM 208S microscope operating at 80 kV. Drops of the sample suspensions (in water) were deposited onto glow-discharged carbon-coated electron microscopy grids, and the excess liquid was absorbed by a piece of filter paper. In order to distinguish the details of samples, a drop of 2 % uranyl acetate negative stain was added before drying. The excess liquid was wiped off, and the remaining film of stain was allowed to dry and kept for observation with TEM.

Scanning electron microscopy (SEM)

The SEM images of typical samples were obtained with a JEOL JSM-5500 Scanning Electron Microscope. Samples were gold coated using an Instrumental Scientific Instrument PS-2 coating unit. The SEM operating voltage was at 15.0 kV.

Thermogravimetric analysis (TGA)

Thermal stability analysis (TGA and DTGA) of the samples was carried out in a Perkin-Elmer (Pyris Diamond) Thermoanalyzer. Samples of pure and modified TOCgel were heated in open platinum pans from 50 to 575 °C, under a nitrogen atmosphere, at a heating rate of 5 °C/min. Then, samples were heated from 575 to 950 °C under air at a heating rate of 15 °C/min.

X-ray photoelectron spectroscopy (XPS)

X-ray photoelectron spectroscopy measurements were performed with a Kratos Ultra electron spectrometer (Kratos Analytical) using a monochromatic AlK ⟨alpha⟩ X-ray source (k = 1486.6 eV) with a power of 225 W, at a take-off angle of 90° relative to the sample surface. The low-resolution survey scans were taken with a 1 eV step and 160 eV analyzer pass energy. High resolution spectra were taken with a 0.1 eV step and 40 eV analyzer pass energy. The analysis area was less than 1 mm^2 and measurements were taken at two different locations on each of the touching faces of pure and modified TOCgel samples surface. The overall spectrum was shifted to ensure that the C–C/C–H contribution to the C1s signal occurred at 285.0 eV. The collected data were analyzed using Vision software version 2.1.3 and CASA XPS version 2.3.

Contact angle measurements (CAM)

Contact angle measurements have been carried out on pellet sample before and after treatment in order to determine the change in wettability. The water sessile drop CAM were carried out on our substrates using an FTA4000Microdrop instrument (First Ten Angstrons, USA) equipped with a CCD camera. All measurements were performed eight times for each sample.

Results and discussion

The TOCgel (up to 90 % nanofibers) used in this study was obtained by selective TEMPO oxidation of primary alcohol groups of wood-cellulose fibers, and followed by a mechanical treatment (defibrillation) [24, 25]. Compared to native cellulose fibers, TOCgel seems to be an innovative nano and bio-material due to the contribution of both the crystalline and amorphous domains present in the structure as illustrated in Fig. 1. The crystalline domain maintained in the structure of cellulose derivative (i.e., TOCgel) could contribute to enhancing the mechanical behavior of composite materials. At the same time, carboxyl (COOH) and hydroxyl (OH) moieties mostly in the amorphous domain

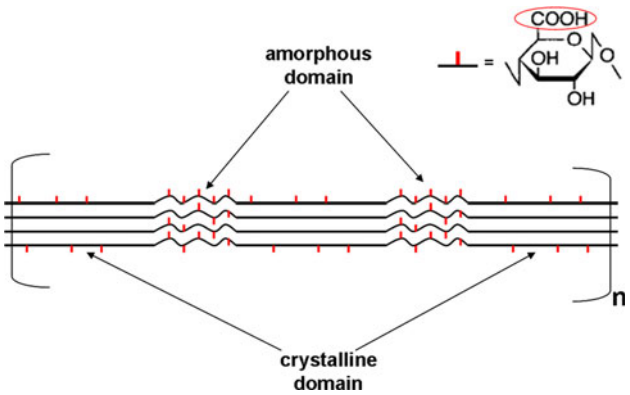

Fig. 1 Schematic illustration of amorphous and crystalline domains in TEMPO-oxidized cellulose gel fibers

make TOCgel highly reactive and consequently improve the covalent linkage during the chemical modification.

In order to render hydrophobic the TOCgel material, these nanofibers were chemically modified by covalent coupling of long carbon chains onto their surface via esterification (O–C=O/alkyl ketene dimer) and amidation (HN–C=O/stearylamine) processes.

In the present work, the efficiency of TOCgel grafting via the both chemical treatments has been presented, then the hydrophobic behavior of the former grafted TOCgels (SA-g-TOCgel and AKD-g-TOCgel) has been investigated in order to compare the final properties of resulting hydrophobized TOCgel fibers.

FTIR and XPS results

Grafting of stearylamine (SA-g-TOCgel)

In the first part of this work, amidation reaction was performed between carboxylate moieties of TOCgel and amine groups of stearylamine using carbodiimide and hydroxysuccimide as catalyst and amidation agent. As mentioned in Fig. 2, FTIR spectra of TOCgel show a large band at 1600–1630 cm^{-1} corresponding to C=O band of carboxylate groups (1610 cm^{-1}) and OH bending of adsorbed water (1635 cm^{-1}), which confirms the oxidation state of native cellulose [28] and the hydrophilic behavior of the TEMPO-oxidized cellulose gel, respectively [31]. After grafting, the success of the amidation was clearly confirmed by the disappearance of carboxylate groups, and the emergence of amide bonding namely amide I at 1645 cm^{-1} (C=O stretching) and amide II at 1545 cm^{-1} (C–N stretching and N–H deformation) [28, 29, 32]. In addition, a substantial increase of the bands at 2860–2940 and 1460 cm^{-1} corresponding to asymmetric and symmetric $–CH_2–$ stretches from long carbon chains of stearylamine was also observed. After grafting, the strong decrease of the peak associated to the vibration of adsorbed

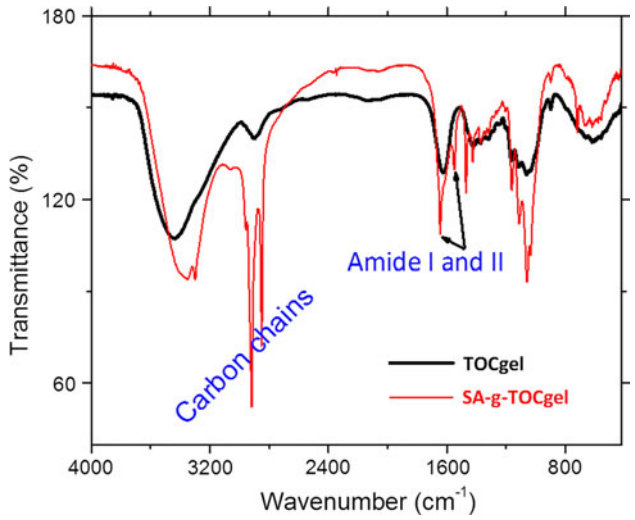

Fig. 2 FTIR spectra of pure TOCgel before and after amidation with SA molecules

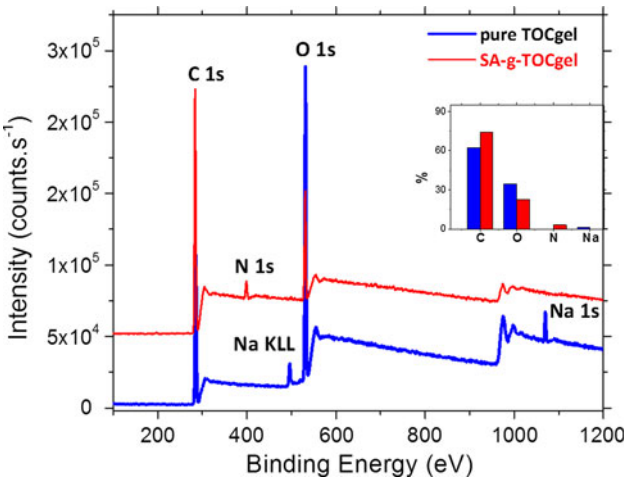

Fig. 3 XPS survey spectra and the corresponding atomic percent values for pure TOCgel and SA-g-TOCgel

water (1635 cm^{-1}) could explain the hydrophobic behavior of the SA-g-TOCgel.

To further prove the grafting of SA chains on TOCgel, X-ray photoelectron spectroscopic study has been used. XPS spectra, shown in Fig. 3, obtained on TOCgel and SA-g-TOCgel surfaces were used to determine the relative C, N, and O content. XPS survey spectra of modified TOCgel show three main peaks, one at 400 eV corresponding to N 1s, one peak at 532 eV corresponding to O 1s, and one peak at 285 eV corresponding to C 1s. The histogram shown in Fig. 3 summarizes the variation in the percentage of atoms of different elements found on the TOCgel surface before and after grafting. The analysis of the corresponding data shows the increase of the nitrogen content from 0 % for the pure TOCgel to up to 3.11 % upon grafting of SA on TOCgel. Furthermore, the decrease in O/C ratio (from 0.56 to 0.3) following the grafting can be attributed to the presence of long aliphatic chains from SA molecules on the one hand, and to the partial removal of oxygen during the formation of the amide bond between COOH of the TOCgel and NH_2 moieties of the SA on the other hand [32, 33]. Moreover, high resolution scans of the XPS spectra of C 1 s and N1 s levels with their respective deconvolutions were also obtained in order to obtain more XPS informations. As shown in Fig. 4a and b, the C 1s XPS spectrum of pure TOCgel can be decomposed into four main components centered at 285.0, 286.7, 288.2, and 289.5 eV. According to the literature [32, 34–36], these moieties were attributed to C1 (C–C/C–H), C2 (C–O), C3 (O–C–O/C=O), and C4 (O–C=O), respectively. Figure 4a and b showed that the intensity of C1 (C–C/C–H) increases strongly from around 27–55 % for TOCgel and SA-g-TOCgel, respectively. Of course, this is the consequence of the strong impact of the long aliphatic chains grafted onto the TOCgel surface. At the same time, the decrease of the C2 component after grafting could be attributed to the elimination of hydroxyl groups of TOCgel during the amidation reaction with the amino group of SA molecules. The shifted value of the binding energy of the C4 component from 289.5 eV (pure TOCgel) to 288.8 eV (after amidation) could be attributed to the presence of covalent bonding (C–N) between the SA molecules and the TOCgel surface. In addition, the occurrence of this amid bound was clearly confirmed in the N 1s spectra as shown in Fig. 4c, with a binding energy of ~399.98 eV. Thus, XPS results clearly confirm the presence of SA chains onto the TOCgel surface.

Grafting of alkyl ketene dimer (AKD-g-TOCgel)

In the second part of this work, esterification reaction was performed between hydroxyl groups of TOCgel and lactone rings of alkyl ketene dimer using 1-methylimidazole as a promoter. As can be seen from the FTIR spectra of TOCgel and AKD-g-TOCgel (Fig. 5), a characteristic band assigned to β-keto ester (around 1704 cm^{-1}) has appeared after esterification indicating that the lactone ring of AKD reacted with hydroxyl groups of TOCgel [37]. Moreover, FTIR spectra also showed the C–H stretching vibration of CH_2 at 2850–2930; 1465 and 725 cm^{-1} indicated the presence of long carbon chains in the molecular structure of the grafted sample. Furthermore, the characteristic absorption peaks at 1060 and 898 cm^{-1} of AKD-g-TOCgel suggested that the molecular structure of the oxidized cellulose did not alter during the reaction in DMAC solvent. In addition, the fact that there was no absorption peak of lactone ring at 1840 cm^{-1} could confirm the removal of unreacted AKD from the final product. Similar to the above results (i.e., amidation), XPS analysis was also used in

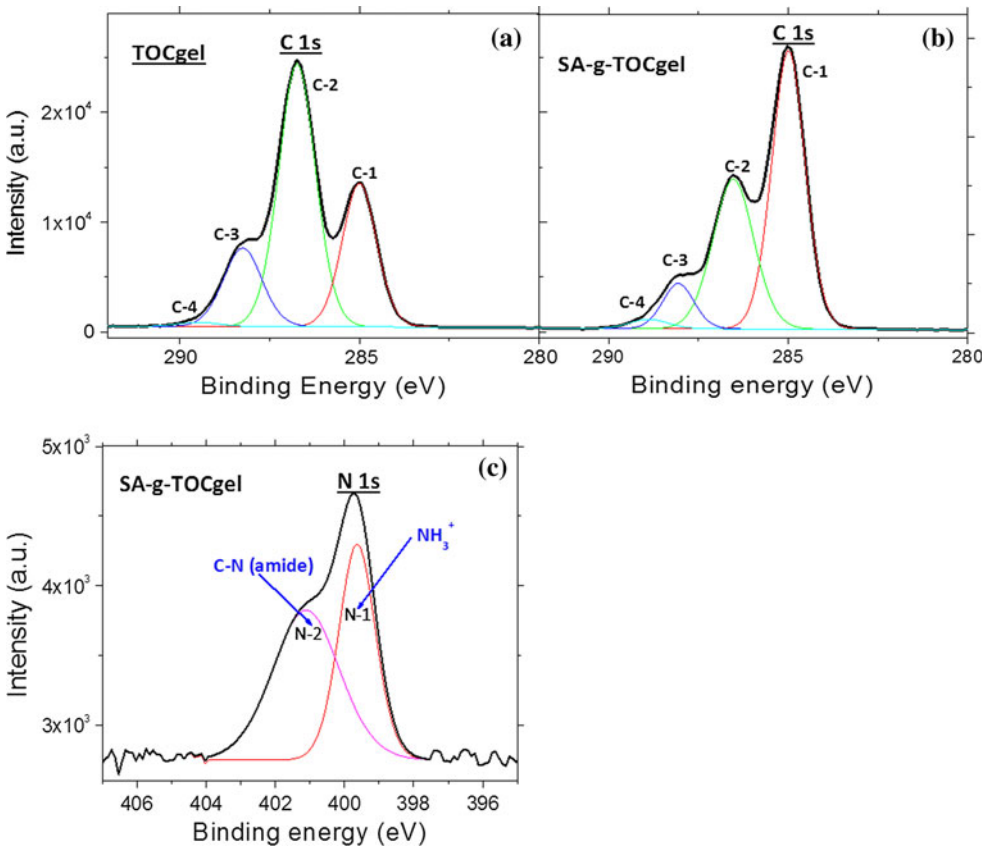

Fig. 4 High resolution spectrum of C 1 s for pure TOCgel and SA-modified TOCgel (**a**, **b**); and of N 1 s for SA-gTOCgel (**c**)

order to confirm the grafting state of the long aliphatic chains of AKD onto the TOCgel surface. Figure 6a shows the XPS survey spectra for TOCgel before and after coupling with AKD. As shown in the survey spectra, Carbon and Oxygen are the predominant species and they occur at 285 and ~533 eV, respectively. However, the most important change was observed for the O/C ratio which decreased from 0.56 for TOCgel to up to 0.21 upon grafting. The decrease in O/C ratio was a clear indication of the attachment of AKD chains on the surface of TOCgel. Of course, this result could be explained by the grafting of long carbon chains of AKD onto the TOCgel surface [33, 38]. At the same time, this result has been confirmed via the high resolution scans of the XPS spectra of C 1s as showed in Fig. 6b. As shown here, the C 1s XPS spectrum of pure TOCgel gives four peaks (C1, C2, C3, and C4) for TOCgel before and after grafting which is in accordance with most data of the literature [34–36]. The intensity of C1 (C–C/C–H) increases strongly from around 27 to 63 % for TOCgel and AKD-g-TOCgel, respectively. This is the consequence of the strong impact of the long aliphatic chains grafted onto the TOCgel surface. Regarding the covalent coupling between AKD (lactone ring) and TOCgel (hydroxyl and/or carboxyl moieties), the esterification was supposed to be occurred with hydroxyl groups of cellulose nanofibers. In this context, the carboxyl amount

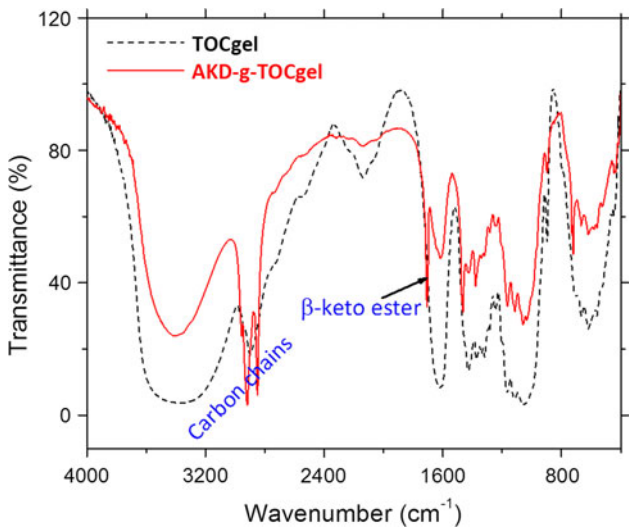

Fig. 5 FTIR spectra of pure TOCgel before and after esterification with AKD molecules

remains almost unchanged even after grafting. However, the decreasing in the intensity of C2 (C–O) from 55 to 31 % as a result of covalent coupling between OH groups of TOCgel and lactone rings of AKD is evidenced by the presence of a discernible band of β-keto ester at 1704 cm^{-1} in FTIR experiment. In addition, the slight increase of the intensity of C4 (O–C=O) could be assigned to the

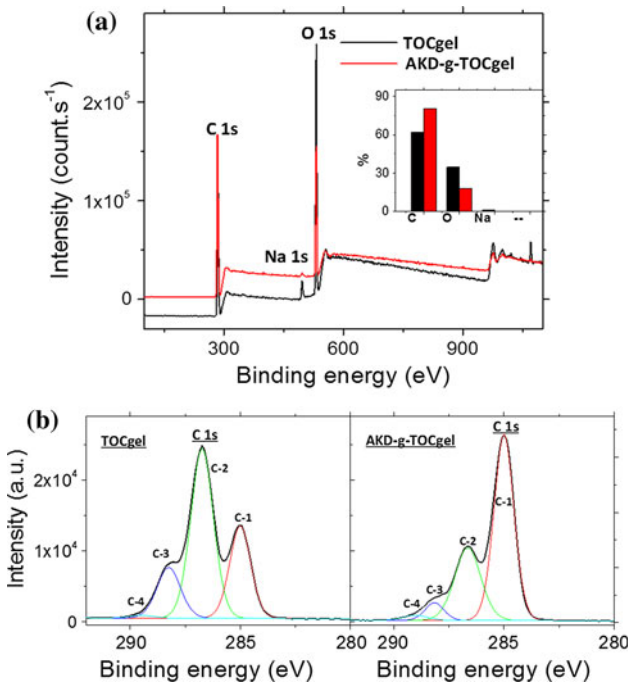

Fig. 6 XPS survey spectra and the corresponding atomic percent values (**a**) and the high resolution spectrum of C 1s (**b**) for pure TOCgel and AKD-g-TOCgel

contribution of the free carboxyl groups of TOCgel (unreacted) and the ester bonds formed after grafting.

Efficiency of TOCgel grafting via the esterification and amidation processes

In order to quantify the grafting state of TOCgel through the both chemical treatments, the graft efficiency of the corresponding modified products was determined.

Referring to Lasseuguette et al. [28], the coupling yield of the amidation product was calculated from (i) the degree of oxidation of the TOCgel before (DO_1) and after (DO_2) coupling with SA molecules and (ii) the degree of coupling (DC) using the electric conductivity titration method and according to the following equation:

$$\text{Coupling Yield}\ (\%) = \left(\frac{\text{DC}}{\text{DO}_1}\right) \times 100 \qquad (1)$$

where $DC = DO_1 - DO_2$

The coupling yield of the SA-g-TOCgel was calculated to be about 85 % which indicates that 85 % of the total amount of carboxyl moieties of TOCgel was covalently coupled with SA molecules.

In this work, the graft efficiency (in term of weight percentage) was calculated using the *gravimetric method* [39, 40] and was about 46.3 % (w/w) according to the following equation:

$$\text{Graft efficiency}(\%) = \left(\frac{\text{m(SA)}}{\text{m(SA)} + \text{m(TOCgel)}}\right) \times 100 \qquad (2)$$

At the same time, the graft efficiency of AKD-g-TOCgel was determined by gravimetric measurements and according to the following equation:

$$\text{Graft efficiency}(\%) = \left(\frac{\text{m(AKD)}}{\text{m(AKD)} + \text{m(TOCgel)}}\right) \times 100 \qquad (3)$$

where $m_{(AKD)}$ (or $m_{(SA)}$) and $m_{(TOCgel)}$ correspond to the mass of the grafted AKD (or SA) and TOCgel, respectively. The corresponding graft efficiency was calculated to be about 30 % (w/w).

TEM images

In order to investigate the effect of the chemical treatment on the morphology and the individualization state of TOCgel fibers, TEM micrographs of our samples were carried out. As showed in Fig. 7, TEM images of TOCgel nanofibers before and after grafting demonstrate that the grafted samples appear to be more entangled than that of pure TOCgel. This result could be attributed to the low surface energy of grafted nanofibers, and consequently to the reduction of their affinity toward the water molecules. Moreover, such result explains the hydrophobic behavior of the final products. The observed entanglement appears to be more pronounced in the SA-g-TOCgel than that of AKD-g-TOCgel which suggested that the amidation process is significantly more effective than the esterification. Using image processing software, the comparison between the fiber width in pure TOCgel (~3 nm) and hydrophobized TOCgel (~4 and 8 nm for SA and AKD treatments, respectively) indicates a slightly increasing of the nanofiber width after grafting. According to earlier published TEM micrographs, this result can be attributed to the adsorbed layers of the hydrophobization agent onto the cellulose nanofiber [28, 33]. In addition, this increase seems to be more important in the case of AKD treatment due to the presence of two long carbon chains in its structure (C14/C16). One can also notice from all micrographs that the morphology of TOCgel nanofibers did not destroyed upon grafting.

Thermogravimetric analysis

The thermogravimetric curves of pure TOCgel before and after grafting are presented in Fig. 8. Both materials contain a few layers of moisture, which were eliminated at 110 °C.

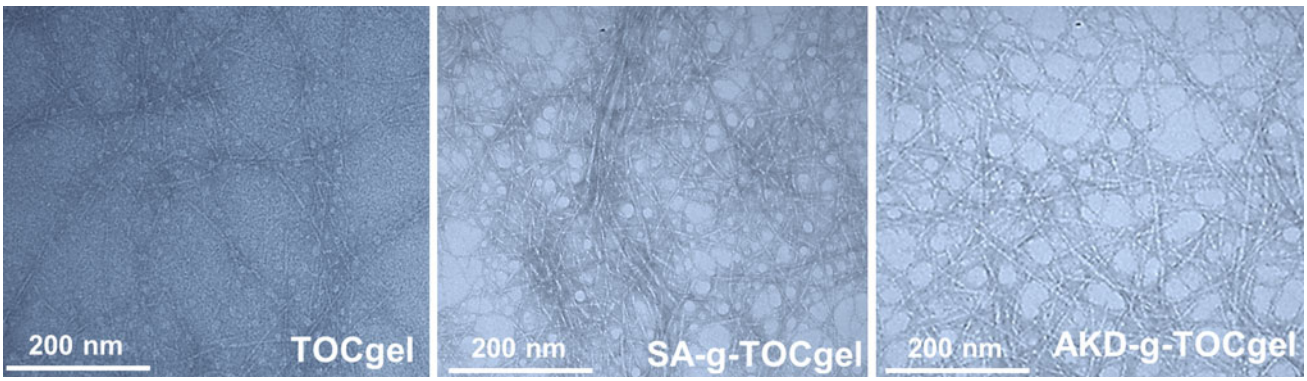

Fig. 7 Transmission electron micrographs of pure TOCgel before and after grafting with SA and AKD molecules

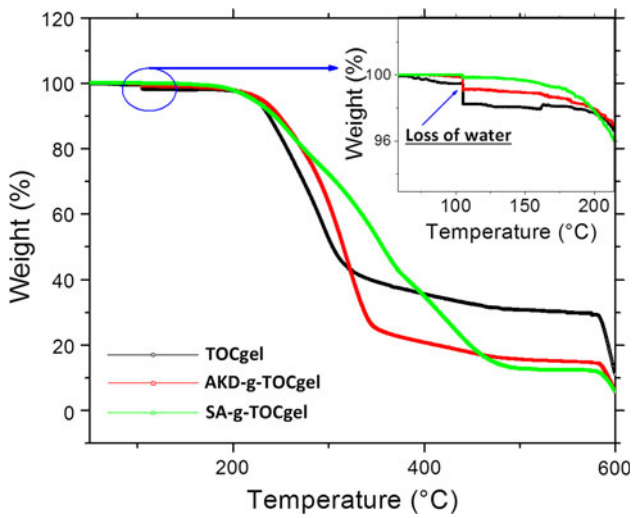

Fig. 8 Thermogravimetric TG curves of pure TOCgel and their corresponding modified samples

As shown in the thermogram curve, pure TOCgel appears to be decomposed between 250 and 293 °C where the corresponding weight loss was attributed to the destruction of the crystalline region of the cellulose nanofiber and decomposition of amorphous region into a monomer of D-glucopyranose and followed by the major thermal-oxidative degradation of polymer chains from 580 °C [41]. In comparison with TG curves of the both SA and AKD grafted TOCgel; results indicate that the hydrophobized TOCgel exhibits higher thermal stability than pure TOCgel which can be clearly highlighted by the ability of the long carbon chains to be organized at the surface to protect TOCgel nanofibers [33]. The covalent coupling between TOCgel and hydrophobized agents (SA or AKD molecules) could explain the shift observed in the thermal degradation temperature of TOCgel from 293 to 316 and 356 °C for AKD-g-TOCgel and SA-g-TOCgel, respectively. The enhanced thermal stability of TOCgel appears to be more pronounced for SA-g-TOCgel than that for AKD-g-TOCgel which, could be explained by the high graft efficiency of amidation process as determined in the paragraph 3.2.

Our results also indicated an increase in the TOCgel hydrophobicity after grafting, as shown in the zoom box in Fig. 8 (zoom) by the decrease of the typical moisture loss around 110 °C (more pronounced for SA-g-TOCgel), suggesting negligible water adsorption, compared with that of the pure TOCgel [42]. This later was confirmed in the FTIR spectra of grafted TOCgel by the strong decrease of the peak associated to the vibration of adsorbed water at 1635 cm^{-1}. Thus, the thermal stability of the composite seems to be clearly increased by the presence of long aliphatic chains grafted onto the fibers surface.

Study of the hydrophobic behavior of grafted TOCgel samples

As presented above in our results, XPS and FTIR spectra confirm clearly the grafting state of TOCgel via chemical treatments with SA and AKD molecules. The graft efficiency was calculated to be about 46.3 and 30 % for SA-g-TOCgel and AKD-g-TOCgel, respectively. At the same time, TEM micrographs demonstrate that the cellulose nanofibers did not altered after grafting.

In this context, it seems to be interesting to point out the hydrophobic behavior of the grafted TOCgel comparing to pure TOCgel. In this context, CAM were performed with water. The high hydrophilic character of pure TOCgel (rich in OH and COOH groups) is well demonstrated by the low contact angle (41° ± 2°) and the corresponding very fast absorption of water drop as indicated in Figs. 9 and 10a, respectively. As shown in Fig. 9, contact angle values of grafted TOCgel are higher than those of the pure TOCgel. Of course, this transition hydrophilic/hydrophobic is ascribed to the nonpolar alkyl chains in the substituents introduced into TOCgel nanofibers. However, this transition seems to be more pronounced for AKD treatment (115° ± 2°) than for SA treatment (102° ± 2°) during the first 30 s of the deposition of the water drop as

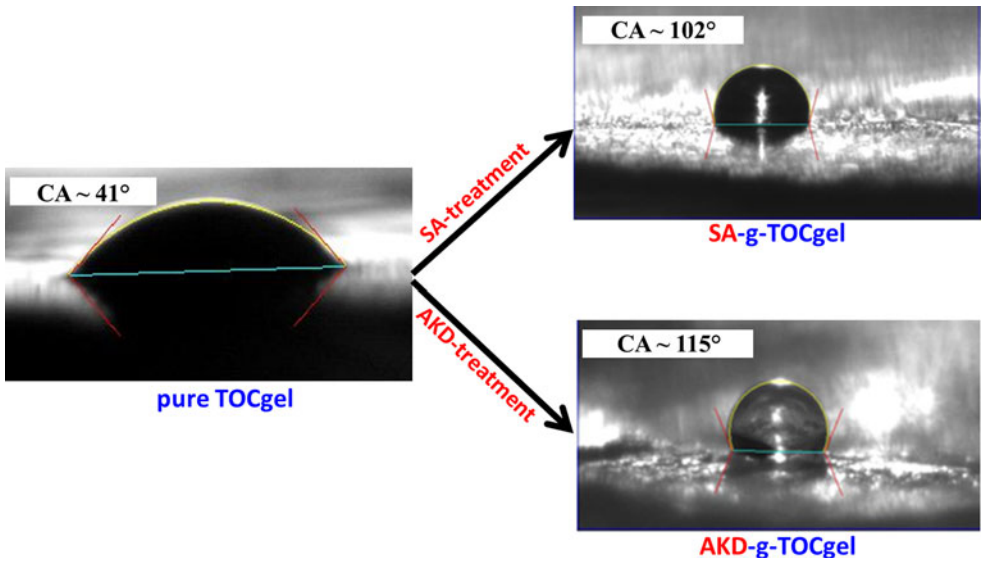

Fig. 9 Contact angles values for pure TOCgel before and after chemical hydrophobization

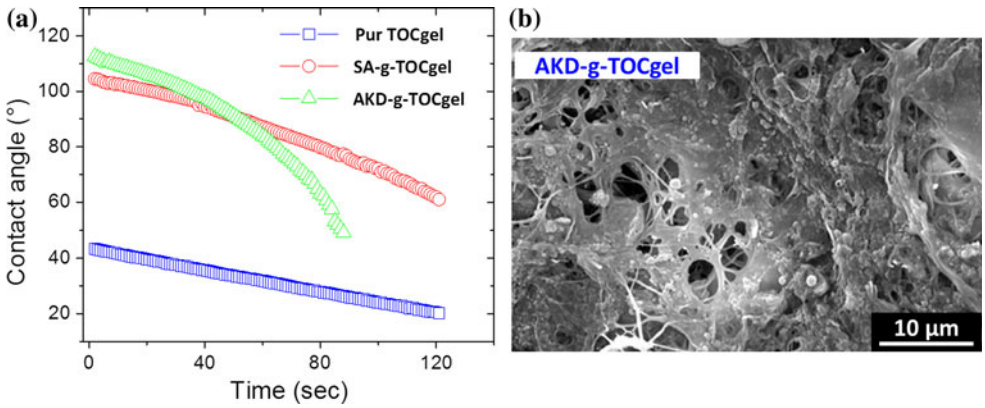

Fig. 10 Contact angle versus time performed with water for pure and grafted TOCgel (**a**); SEM micrograph of AKD-g-TOCgel showing the granular features of AKD microparticles (**b**)

demonstrated in Fig. 10a. Moreover, the loss of hydrophobicity of the both modified TOCgel fibers was also followed by measurement of the decrease in contact angle value of a water drop deposited on the fibers as a function of time. As can be seen from this result, the contact angle decreased progressively versus time, and the absorption of water drop by the fibers appears to be slow for SA-g-TOCgel than for AKD-g-TOCgel. The slightly greater contact angles for the AKD-g-TOCgel may be explained by the higher surface roughness of the pellet sample. Furthermore, the granular feature of AKD-g-TOCgel surface showed in Fig. 10b gives an additional roughness to its surface and consequently, contributes to the increase of its contact angle value. Moreover, the water absorption phenomenon observed for the both modified TOCgel fibers versus time, suggesting that a sufficient number of residual polar groups (i.e., –OH, COOH) had been regenerated under it and thus facilitated its capillary penetration. However, the higher absorption rate of water drop into the fibrous network of AKD-g-TOCgel more than of SA-g-TOCgel (even after 30 s) could be explained by (i) the higher graft efficiency (~46.3 %) which indicates the protective role of long aliphatic chains even well organized onto the cellulose nanofibers in the former SA-g-TOCgel and (ii) the grafting of colloidal microparticles of AKD on TOCgel fibers which could hinder the diffusion of other AKD molecules into the bulk of the materials, and consequently contribute to a low graft efficiency (~30 %) for the AKD-g-TOCgel. This result was confirmed by the dispersion test of modified TOCgel in non-polar solvent like hexane as showed in Figs. 11 and 12. As can be seen from these pictures, pure TOCgel is unstable in hexane and a flocculation phenomenon was observed. After chemical modification, SA-g-TOCgel fibers seem to be homogeneously dispersed (stable) in the hexane solution that becomes turbid after the migration of the long alkyl chains into the nonpolar phase. However, the dispersion of AKD-g-TOCgel fibers appears to be less stable in hexane solution which could be explained by the low graft efficiency of the esterification process. Based on the above comparative

study between the both chemical treatments, several assumptions can be proposed: (i) The dimensions of dispersed colloidal AKD particles (about 1 μm) could affect their accessibility toward the hydroxyl groups of TOCgel nanofibers and consequently, hinder the diffusion of other AKD particles to be grafted into the bulk of the material. This explanation could be responsible to the low graft efficiency of the AKD-g-TOCgel. In addition, AKD is supposed to react with the hydroxyl moieties of the TOCgel. However, the hydrogen bonds in the TOCgel fibrous network could impede in some case, the occurrence of the esterification process between the lactone rings of AKD and the cellulose nanofibers. (ii) In the amidation process, carboxylate moieties of TOCgel are totally accessible to form amide bonds with amine groups of SA molecules. In addition, the smaller size of SA in comparison with that of AKD particles could facilitate the diffusion of SA chains toward the bulk of TOCgel network and explain the high graft efficiency of the amidation reaction. Despite all, work is in progress in order to investigate quantitatively the chemical effect of ester bonds versus amide bonds on the chemical stability of modified cellulose fibers.

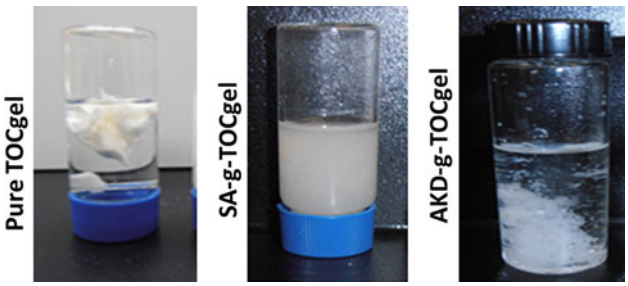

Fig. 11 Dispersion tests of samples in hexane solvent

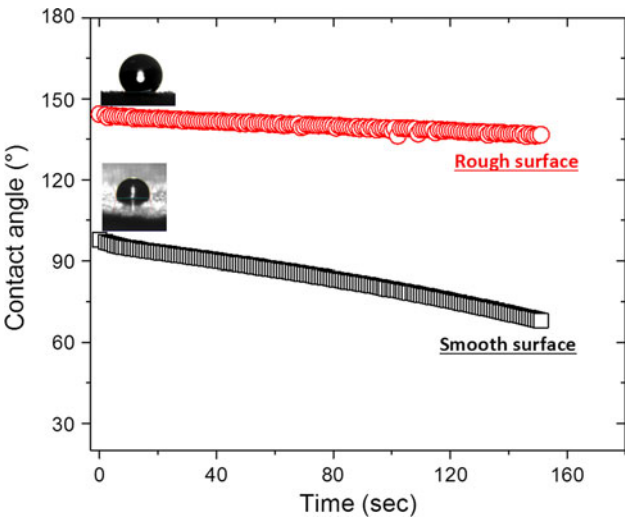

Fig. 12 Evolution of contact angle versus time for smooth and rough hydrophobized TOCgel surfaces

Thanks to the good hydrophobic behavior of our modified materials, it seems interesting to point out the possibility to get a superhydrophobic surface with these SA or AKD modified cellulose nanofibers. Recently, the creation of superhydrophobic, self-cleaning, cellulose-fiber-based materials will have potential applications in the textile industry and packaging area [3]. In our presented result, CAM were realized on pellet sample (compressed fibers) having a smooth surface. This is advantageous in the comparison of the CA values between SA and AKD modified TOCgel.

In this context, CAM were tested directly on freeze dried films of SA-g-TOCgel (rough surface), and the surface wettability of these substrates has been assessed by a series of CAM versus time. Figure 11 showed clearly a transition to a stable superhydrophobic surface (around 150°) which indicates the strong effect of the roughness on the contact angle according to the Cassie–Baxter equation [43]. Moreover, this superhydrophobicity could be attributed to the association of the fraction of air trapped in the rough surface of porous SA-g-TOCgel and usage of low surface energy coating.

Conclusions

In conclusion, stearylamine and alkyl ketene dimer were successfully grafted onto the surface of TOCgel nanofibers via the formation of amide and β-keto ester bonds, respectively, under heterogeneous conditions. Covalent coupling onto the TOCgel surface was clearly confirmed by XPS, FTIR, TEM, and CAM. In addition, the graft efficiency of the final product was determined to be about 46.3 % (w/w) for SA-modified TOCgel and 30 % (w/w) for AKD-g-TOCgel which suggested a high efficiency of the amidation versus the esterification in the chemical modification of oxidized cellulose nanofibres. This result appears to be advantageous to explain the high water resistance of SA-g-TOCgel comparing to that of AKD-g-TOCgel. Based on the TEM images, the nanofibrillar structure of the TOCgel was preserved after the both chemical treatments. Results showed also that the thermal stability of TOCgel was enhanced after grafting and appeared to be more pronounced for the SA-g-TOCgel which could be explained by the higher graft efficiency of SA molecules well organized onto nanofibers surface. In addition, the possibility to obtain a superhydrophobic TOCgel surface (∼150°) was discussed based on the surface roughness of the modified TOCgel. The excellent hydrophobic properties of the modified TOCgel materiel could be suitable to be used as reinforcement for nonpolar polymer matrices for several applications. Work is in progress in order to investigate quantitatively the chemical

effect of ester bonds versus amide bonds on the efficiency and chemical stability of hydrophobic cellulose nanofibers.

Acknowledgements The authors gratefully acknowledge the Natural Science and Engineering Research Council of Canada (NSERC) for financial support.

References

1. Azizi Samir MA, Alloin F, Dufresne A (2005) Review of recent research into cellulosic whiskers, their properties and their application in nanocomposite field. Biomacromolecules 6:612–626
2. Orts WJ, Shey J, Imam SH, Glenn GM, Guttman ME, Revol JF (2005) Application of cellulose microfibrils in polymer nanocomposites. J Polym Environ 13:301–306
3. Klemm D, Heublein B, Fink HP, Bohn A (2005) Cellulose: fascinating biopolymer and sustainable raw material. Angew Chem Int Ed 44:3358
4. Czaja WK, Young DJ, Kawecki M, Brown RM Jr (2007) The future prospects of microbial cellulose in biomedical applications. Biomacromolecules 8(1):1
5. Siqueira G, Bras J, Dufresne A (2009) Cellulose whiskers versus microfibrils: influence of the nature of the nanoparticle and its surface functionalization on the thermal and mechanical properties of nanocomposites. Biomacromolecules 10(2):425–432
6. Gradwell SE, Renneckar S, Esker AR, Heinze T, Gatenholm P, Vaca-Garcia C, Glasser W (2004) Surface modification of cellulose fibers: towards wood composites by biomimetics. CR Biol 327(9–10):945–953
7. Baiardo M, Frisoni G, Scandola M, Licciardello A (2002) Surface chemical modification of natural cellulose fibers. J Appl Polym Sci 83(1):38–45
8. Belgacem M, Gandini A (2005) The surface modification of cellulose fibres for use as reinforcing elements in composite materials. Compos Interfaces 12:41–75
9. Bledzki AK, Gassan J (1999) Composites reinforced with cellulose based fibers. Prog Polym Sci 24:221–274
10. Tingaut P, Zimmermann T, Lopez-Suevos F (2010) Synthesis and characterization of bionanocomposites with tunable properties from poly(lactic acid) and acetylated microfibrillated cellulose. Biomacromolecules 11(2):454–464
11. Lonnberg H, Zhou Q, Brumer H, Teeri TT, Malmstrom E, Hult A (2006) Grafting of cellulose fibers with poly(e-caprolactone) and poly(L-lactic acid) via ring-opening polymerization. Biomacromolecules 7(7):2178–2185
12. Roy D, Guthrie JT, Perrier S (2005) Graft polymerization: grafting poly(styrene) from cellulose via reversible addition-fragmentation chain transfer (RAFT) polymerization. Macromolecules 38(25):10363–10372
13. Carlmark A, Malmstrom E (2003) ATRP grafting from cellulose fibers to create block-copolymer grafts. Biomacromolecules 4(6):1740–1745
14. Coskun M, Temüz MM (2005) Grafting studies onto cellulose by atom-transfer radical polymerization. Polym Int 54(2):342–347
15. Gaiolas C, Belgacem MN, Silva L, Thielemans W, Costa AP, Nunes M, Silva MJS (2009) Green chemicals and process to graft cellulose fiber. J Colloid Interface Sci 330(2):298–302
16. Ly B, Bras J, Sadocco P, Belgacem MN, Dufresne A, Thielemans W (2010) Surface functionalization of cellulose by grafting oligoether chains. Mater Chem Phys 120(2–3):438–445
17. Benkaddour A, Jradi K, Robert S, Daneault C (2013) Grafting of polycaprolactone on oxidized nanocelluloses by click chemistry. Nanomaterials 3:141–157
18. Lin N, Huang J, Dufresne A (2012) Preparation, properties and applications of polysaccharide nanocrystals in advanced functional nanomaterials. Nanoscale 11(4):3274–3294
19. Chanzy H (1990) Aspects of cellulose structure. In: Kennedy JF, Philips GO, William PA (eds) Cellulose sources and exploitation. Ellis Horwood Ltd, New York, p 3–12
20. Marchessault RH, Morehead FF, Walter NM (1959) Liquid crystal systems from fibrillar polysaccharides. Nature 184:632
21. Kim J, Yun S, Ounaies Z (2006) Discovery of cellulose as a smart material. Macromolecules 39:4202
22. Paakko M, Ankerfors M, Kosonen H, Nykanen A, Ahola S, Osterberg M, Ruokolainen J, Laine J, Larsson PT, Ikkala O, Lindstrom T (2007) Enzymatic hydrolysis combined with mechanical shearing and high-pressure homogenization for nanoscale cellulose fibrils and strong gels. Biomacromolecules 8:1934
23. Elazzouzi-Hafraoui S, Nishiyama Y, Putaux JL, Heux L, Dubreuil F, Rochas C (2008) The shape and size distribution of crystalline nanoparticles prepared by acid hydrolysis of native cellulose. Biomacromolecules 9:57
24. Saito T, Nishiyama Y, Putaux JL, Vignon M, Isogai A (2006) Homogeneous suspensions of individualized microfibrils from TEMPO-catalyzed oxidation of native cellulose. Biomacromolecules 7:1687
25. Loranger E, Piché AO, Daneault C (2012) Influence of high shear dispersion on the production of cellulose nanofibers by ultrasound-assisted TEMPO-oxidation of kraft pulp. Nanomaterials 2(3):286–297
26. Loranger E, Paquin M, Daneault C, Chabot B (2011) Comparative study of sonochemical effects in an ultrasonic bath and in a large-scale flow-through sonoreactor. Chem Eng J 178:359–365
27. Okita Y, Saito T, Isogai A (2010) Entire surface oxidation of various cellulose microfibrils by TEMPO-mediated oxidation. Biomacromolecules 11:1696
28. Lasseuguette E (2008) Grafting onto cellulose microfibrils. Cellulose 15:571–580
29. Araki J, Wada M, Kuga S (2001) Steric stabilization of a cellulose microcrystal suspension by poly(ethylene glycol) grafting. Langmuir 17:21
30. Johnson RK, Zink-Sharp A, Glasser WG (2011) Preparation and characterization of hydrophobic derivatives of TEMPO-oxidized nanocellulose. Cellulose 18:1599–1609
31. Oh SY, Yoo DI, Shin Y, Seo G (2005) FTIR analysis of cellulose treated with sodium hydroxide and carbon dioxide. Carbohydr Res 340:417–428
32. Barazzouk S, Daneault C (2012) Tryptophan-based peptides grafted onto oxidized nanocellulose. Cellulose 19:481–493
33. Missoum K, Bras J, Belgacem MN (2012) Organization of aliphatic chains grafted on nanofibrillated cellulose and influence on final properties. Cellulose 19:1957–1973
34. Kamdem DP, Zhang J, Adnot A (2001) Identification of cupric and cuprous copper in copper naphthenate-treated wood by X-ray photoelectron spectroscopy. Holzforschung 55:16–20
35. Johansson LS, Campbell JM (2004) Reproducible XPS on biopolymers: cellulose studies. Surf Interface Anal 36:1018–1022
36. Ahmed A, Adnot A, Grandmaison JL, Kaliaguine S, Doucet J (1987) ESCA analysis of cellulosic materials. Cellulose Chem Technol 21(5):483–492
37. Song X, Chen F, Liu F (2012) Preparation and characterization of alkyl ketene dimer (AKD) modified cellulose composite membrane. Carbohydr Polym 88:417–421
38. Matuana LM, Balatinecz JJ, Sodhi RNS, Park CB (2001) Surface characterization of esterified cellulosic fibers by XPS and FTIR Spectroscopy. Wood Sci Technol 35:191–201
39. Habibi Y, Goffin AL, Schiltz N, Duquesne E, Dubois P, Dufresne A (2008) Bionanocomposites based on poly(3-caprolactone)-

grafted cellulose nanocrystals by ring-opening polymerization. J Mater Chem 18:5002–5010
40. Littunen K, Hippi U, Johansson LS, Österberg M, Tammelin T, Liane J, SeppäläJ (2011) Free radical graft copolymerization of nanofibrillated cellulose with acrylic monomers. Carbohydr Polym 84:1039–14047
41. Rambo CR, Recouvreux DOS, Carminatti CA, Pitlovanciv AK, Antonio RV, Porto LM (2008) Template assisted synthesis of porous nanofibrous cellulose membranes for tissue engineering. Mater Sci Eng C 28:549
42. Cunha AG, Freire CSR, Silvestre AJD, Neto CP, Gandini A, Orblin E, Fardim P (2007) Highly hydrophobic bio- polymers prepared by the surface pentafluorobenzoylation of cellulose substrates. Biomacromolecules 8:1347–1352
43. Cassie ABD, Baxter S (1944) Wettability of porous surfaces. Trans Faraday Soc 40:546–551